P1.1

Forecasting of the winds along the glide paths at an airport by applying a chaotic oscillatory neural network (CONN) to the Doppler LIDAR data

K.M. Kwong
Hong Kong Polytechnic University

P.W. Chan *
Hong Kong Observatory, Hong Kong, China

1. INTRODUCTION

The complex terrain in the vicinity of the Hong Kong International Airport (HKIA) may lead to low-level windshear and turbulence (below 1600 feet) affecting the arriving/departing aircraft. To monitor these wind disturbances which mostly occur in non-rainy weather conditions, Doppler LIght Detection and Ranging (LIDAR) systems are operated by the Hong Kong Observatory (HKIA). For more efficient monitoring, the LIDARs have been configured to scan along the glide paths of the aircraft in making wind measurements. The Doppler velocities collected in this "glide path scan" are used to construct the headwind profile to be encountered by the aircraft, from which significant wind changes are detected automatically in the issuance of windshear alerts (Shun and Chan, 2008). They have also been used in experiments to calculate the spatial distribution of turbulence intensity along the glide paths (Chan and Kwong, 2008).

The above applications of the LIDARs aim at *detecting* windshear and turbulence when they arise. The next step would be the *forecasting* of such phenomena given the latest wind conditions along the glide paths as shown in the LIDAR data. The forecasting could involve numerical weather prediction (NWP) models which are based on all the physical equations governing the evolution of the atmosphere. In Kwong and Chan (2008), an alternative approach is adopted, namely, the application of a chaotic oscillatory-based neural network (CONN) to the LIDAR data. The evolution of the wind field over a 2D region (namely, a scanning sector by the LIDAR) is considered in that paper, and the wind vector at a particular location within the 2D region in the future is supposed to be related to the winds at the neighbouring positions in the past. While this method takes into account the winds over a wider area (e.g. wind vectors upstream of the location in question and thus advection of the wind disturbances across the location by the "prevailing" wind), both the training and the prediction are computationally expensive, thus prohibiting the use of a training dataset over a longer period and the prediction for a longer time. For instance, in Kwong and Chan (2008), training of CONN is limited to the LIDAR data in the last several hours only, which most probably has not covered the wind features to be predicted. As a result, there is a compromise between the amount of data to be input into CONN and the period of training dataset due to computational constraint.

The present paper considers another approach in the application of CONN, namely, focusing on the wind data along the glide path only (and thus a 1D problem instead of 2D) whilst extending the period of the training dataset (in the order of days). With the use of a 1D approach, it is thus assumed that the wind at a particular location along the glide path in the future is related to the winds along the whole glide path in the past in a certain way. This assumption is considered to be a much simplified view of the wind field evolution compared to the 2D approach in Kwong and Chan (2008), but the advantage is that it allows the wind data collected by glide path scans over a much longer period to be used in the training of the neural network, which has a higher chance to cover the wind features to be predicted. The structure of CONN used in the present study is described in Section 2. Examples of wind predictions are given in Section 3.

A number of tuning of CONN has been tried out in the present study, namely, the choice of averaging method of the CONN-output wind profiles, the number of neurons in the hidden layer and the ordering of the training data. They are described in Sections 4 to 6. A longer forecasting time has also been considered, as described in Section 7. Section 8 gives the conclusions of this study.

2. STRUCTURE OF CONN

The wind data (Doppler velocity) along the whole glide path at each time instance is input into CONN. The output of CONN is also the winds along the glide path but at a future time, and the neural network learns from the root-mean-square difference between the predicted wind data and the actually measured wind data by the LIDAR through back propagation. In the testing process, the neural network uses the experience gained in the training process to generate the forecast for the next time interval(s). The structure of CONN is schematically shown in Figure 1.

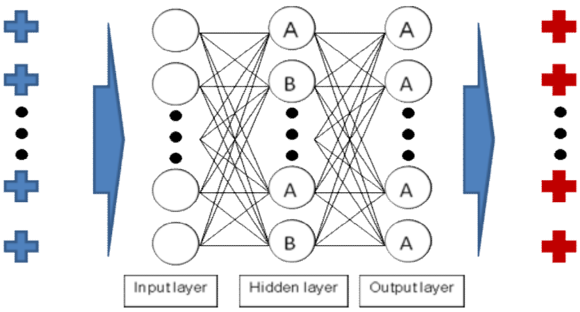

Figure 1 Structure of CONN

CONN in the present study is made up of a multi-layered perception (MLP) neural network and a

* *Corresponding author address:* P.W. Chan, Hong Kong Observatory, 134A Nathan Road, Hong Kong
email: pwchan@hko.gov.hk

Lee Oscillator (Retrograde Transport) with different sets of parameter settings. Details of the Lee Oscillator could be found in Kwong and Chan (2008). In the hidden and output layers, two different parameter settings of the Lee Oscillator have been used. Their bifurcation diagrams are shown in Figure 2. The idea is to use a combination of two oscillators with different degree of oscillations (smaller oscillation for type A and greater oscillation for type B).

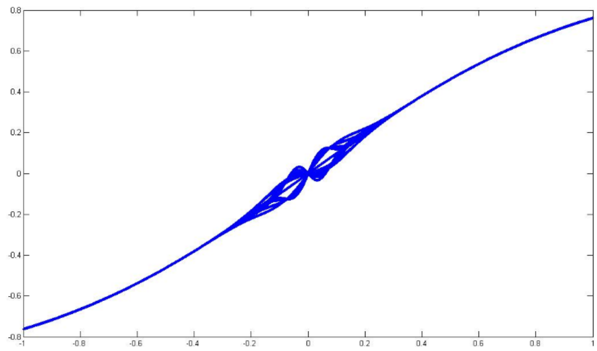

(a)

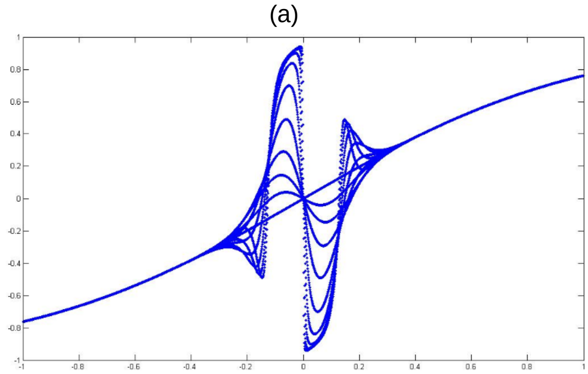

(b)

Figure 2 Bifurcation diagrams of Lee Oscillator (Retrograde Transport) with parameter setting A (a) and B (b).

3. EXAMPLES OF PREDICTION

Two cases are considered in this paper. In the first case, easterly winds prevailed at HKIA and mountain wake flow appeared to the southwest of the airport, as shown from the LIDAR measurement of the wind (Figure 3(a)). An aircraft landing at the south runway from the west (the 07RA runway corridor, location in Figure 3(a)) conducted missed approach at 04:20 UTC on that day due to encountering of significant windshear. The headwind profiles measured by the LIDAR over this runway corridor around the event time are given in Figure 3(c)). Training of CONN is conducted using the 07RA headwind profiles from 00 UTC, 16 March to 03 UTC, 20 March 2006. Forecasting is then made from 03:02 UTC to 04:33 UTC, 20 March 2006. The forecast at time 03:02 UTC is based on the LIDAR data at 03:00 UTC, the forecast at 03:06 UTC is based on the data at 03:02 UTC, and so on. The forecast results are shown in Figure 3(e). It could be seen that, though the forecast headwind change is smaller than reality (see the wind changes in Figure 3(c) vs. Figure 3(e)), the occurrence of windshear between 0.6 and 1 nautical mile away from the runway end in the period of about 04:00 to 04:30 UTC has been successfully captured.

The second case is wind change due to sea breeze in autumn. Sea breeze is also a major cause of low-level windshear at HKIA. Once again, the runway corridor 07RA is considered. Easterly winds prevailed over HKIA on that day and westerly sea breeze set in to the west of the airport in late morning, as depicted by the LIDAR measurement (Figure 3(b)). The evolution of headwind profiles over 07RA is shown in Figure 3(d). In CONN, the LIDAR's glide-path scan data over 07RA in the period 00 UTC, 24 October to 02 UTC, 28 October 2007 are used in the training. Forecast is made from 02 UTC to 03 UTC, 28 October 2007 in the same way as the first case. The forecast result is shown in Figure 3(f). Once again, CONN successfully captures the headwind change from 0.7 to 1.1 nautical miles from the runway end between 02:30 and 03:00 UTC on that day. Compared to the actual measurements, the forecast headwind change appears to be a little bit less abrupt (i.e. a smaller slope of headwind change with distance from the runway threshold).

Tuning of CONN and a trial of a longer forecasting period have been tried out. The results are discussed in Sections 4 to 7. In these studies, only the sea breeze case on 28 October 2007 has been considered, as a first step. More cases would be considered in further studies.

4. CHOICE OF AVERAGING METHOD

The forecast headwind profiles in Figure 3(e) and (f) seem to be rather noisy. Part of the noise arises from numerical computation, which may be exaggerated by the Lee Oscillator. For comparison purpose, the forecast for the sea breeze case has been made with the traditional MLP in which hyperbolic tangent threshold function is employed. For the CONN forecasts, a number of variants has been tried out, including:

(a) CONN forecast is made for a particular single run;
(b) a total of 15 forecasts of the wind field is made for the following few minutes and their arithmetic average is taken;
(c) a total of 15 forecasts is made, two extreme wind forecasts removed and the average of the remaining 13 headwind profiles taken;
(d) the median of the 15 forecasts is made.

The resulting forecasts are shown in Figure 4. Compared to the result of a single run, the use of traditional MLP and the smoothing of CONN forecasts produce less noisy headwind profiles. The quality of the forecast wind data is studied by calculating correlation coefficient with the actually measured headwind profiles. The performance statistics are shown in Table 1. It turns out that the use of arithmetic average of the 15 CONN forecasts (i.e. method (b)) gives the highest correlation coefficient on average.

5. NUMBER OF NEURONS IN THE HIDDEN LAYER

There is no general rule about the optimal number of neurons in the hidden layer for a neural network to give the best forecast, but this is rather a matter of trial and error for the particular problem under study (Zhang et al., 1998). As a tuning of CONN for the present study, the number of neurons in the hidden layer has been varied between 5 and 9 for the sea breeze case. The forecast headwind profiles for different number of neurons are shown in Figure 5. There are slight differences in the forecast results. For instance, for the headwind profile at 02:58 UTC, 28 October 2007, the use of more neurons in the hidden layer appears to cause the resulting profile to become more or less "flattened" (i.e. relatively small change of headwind with distance away from the runway threshold) at an increasing distance from the runway end, from about 1.1 nautical mile for 5 neurons to about 1.3 nautical mile for 9 neurons. Compared with the actual measurement (Figure 3(f)), a choice of 7 – 8 neurons seems to give the most reasonable forecast.

6. ORDERING OF THE TRAINING DATA

It would be interesting to see if the CONN forecast is related to the ordering of the wind data in the training dataset. For the sea breeze case, the LIDAR data between 24 and 28 October 2007 have been used in the training of CONN. The wind data between 00 UTC of a day in this period up to 00 UTC of the following day is taken as a data chuck, and the four data chucks are permuted in each training process. Only the data between 00 and 02 UTC, 28 October 2007 remain as the last part in the training dataset. The forecast result of one such permutation is shown in Figure 6. The headwind change associated with the sea breeze is still successfully captured. It appears that the ordering of the training data, at least the period from 00 UTC of a day to the same time of the following day is preserved, does not significantly affect the forecasting of the main feature in the headwind change.

7. FORECASTING FOR A LONGER TIME

In the previous discussion, the forecasting is made by steps of every few minutes or so. The possibility of having a longer forecasting period is considered, namely:

(a) Skip 4 – The first 4 scans (lasting 7-8 minutes) in the forecast period are not considered, so that data at 02:00 UTC is used to forecast the time 02:07 UTC, data at 02:02 UTC is used to forecast the time 02:09, etc.
(b) Skip 7 – The first 7 scans (lasting 13-14 minutes) are not considered, so that data at 02:00 UTC is used to forecast the time 02:13 UTC, data at 02:02 UTC is used to forecast the time 02:14, etc.
(c) Skip 8 – The first 8 scans are not considered.
(d) Skip 16 – The first 16 scans are not considered.

The results are shown in Figure 7. It could be seen that with a larger number of scans to be skipped, the headwind change pattern associated with sea breeze becomes less apparent. Considering all the results, it looks like no skipping of the scans produces the best results, and skipping would cause the quality of wind forecast to progressively deteriorate.

8. CONCLUSIONS

Wind forecasting using CONN over a glide path of the airport is demonstrated in this paper. Two typical cases of low-level windshear have been considered, namely, terrain-disrupted airflow and sea breeze. For the limited number of cases being studied, it appears that CONN has some skills in forecasting the headwind changes. With the use of the sea breeze case, the CONN forecasting method has been tuned, e.g. in the choice of averaging method to minimize the computational noise and the determination of the number of neurons in the hidden layer. The ordering of the wind data in the training dataset (at least for permutation of data of different days) does not seem to significantly affect the capturing of the major headwind change feature. Finally, forecast for a longer time period has been considered by skipping the first 4 to 16 scans in the forecast period, but the result does not seem to be promising with the increasing number of scans to be skipped. More windshear and turbulent flow cases captured by the LIDARs at HKIA would be used to further study the wind forecasting capability of the CONN proposed in this paper, especially for the more challenging cases of flow disruption by terrain.

References

Chan, P.W., and K.M. Kwong, 2008: Performance of LIDAR-based turbulence detection algorithm. *13th Conference on Aviation, Range and Aerospace Meteorology*, New Orleans, Louisiana, USA, 20-24 January 2008.

Kwong, K.M., and P.W. Chan, 2008: Short-term wind forecasting at the Hong Kong International Airport by applying chaotic oscillatory-based neural network to LIDAR Data. *13th Conference on Aviation, Range and Aerospace Meteorology*, New Orleans, Louisiana, USA, 20-24 January 2008.

Shun, C.M., and P.W. Chan, 2008: Applications of an infrared Doppler LIDAR in detection of windshear. *J. Atmos. Oceanic Technol.*, **25**, 637-655

Zhang, G., B.E. Patuwo, and M.Y. Hu, 1998: Forecasting with artificial neural networks: The state of the art. International Journal of Forecasting, **14**, 35-62.

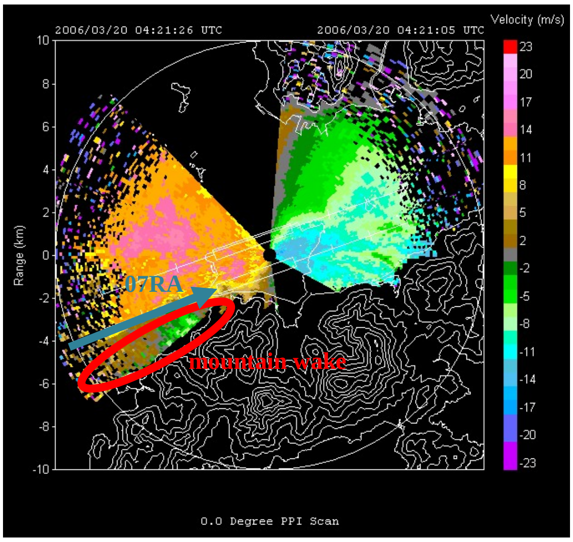

(a) LIDAR velocity imagery of spring-time easterly wind case with mountain wake

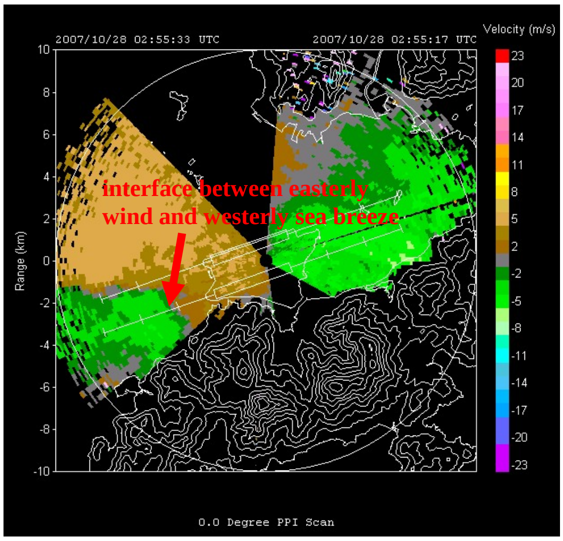

(b) LIDAR velocity imagery of sea breeze case

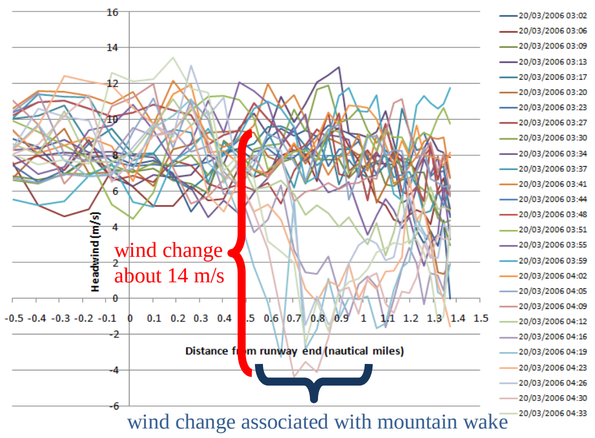

(c) the headwind profiles over western approach to south runway as measured by the LIDAR for the spring-time easterly wind case

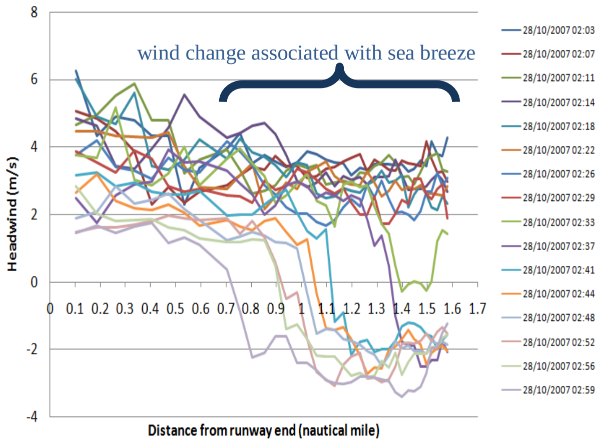

(d) the headwind profiles over western approach to south runway as measured by the LIDAR for the sea breeze case

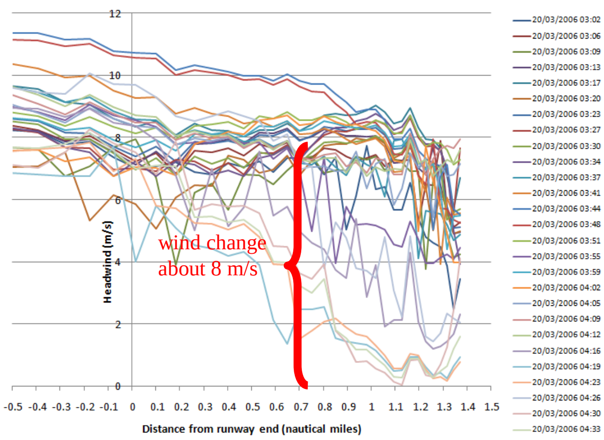

(e) the predicted headwind profiles based on CONN for the spring-time easterly wind case

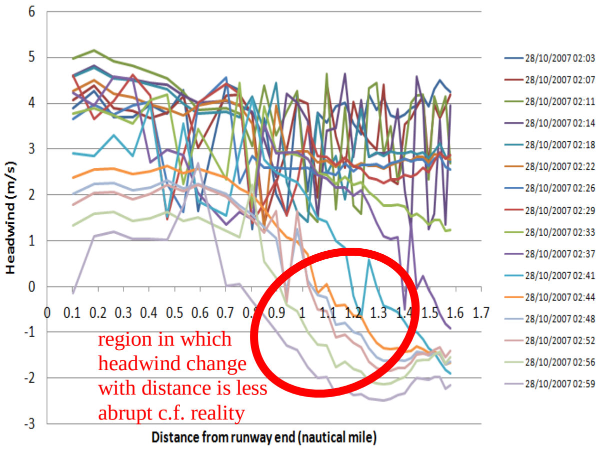

(f) the predicted headwind profiles based on CONN for the sea breeze case

Figure 3 LIDAR velocity imagery and headwind profiles for the two cases under study in Section 3.

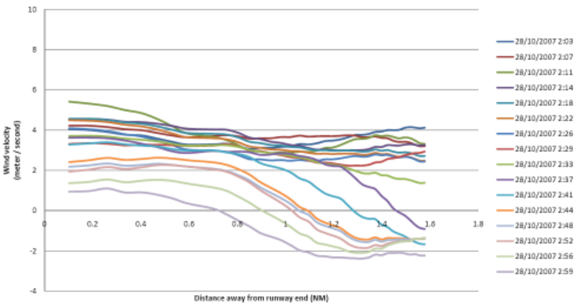

MLP

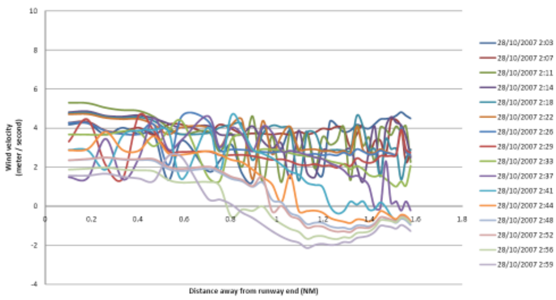

Single run using CONN

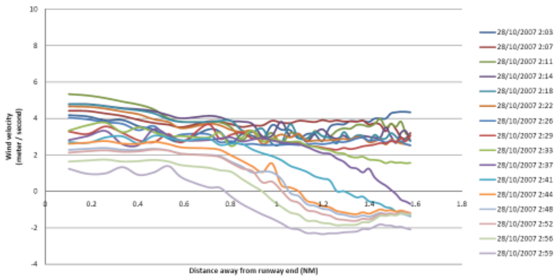

Average of15 trials using CONN

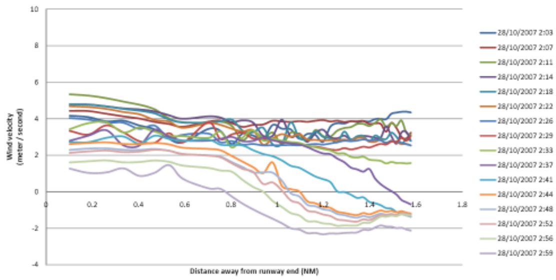

Removal of the two extremes based on CONN

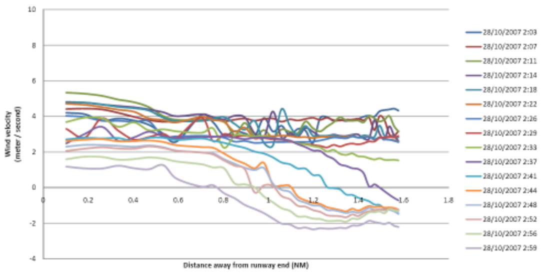

Median of CONN forecasts

Figure 4 Results of different averaging methods for CONN forecasts

Time (UTC)	MLP Neural Network	CONN (Single trial)	CONN (Average of 15 Trials)	CONN (Averaged with removing the two extreme)	CONN (Median of 15 Trial)
28/10/2007 2:03	0.279557	0.668751	0.381582	0.377894	0.371066
28/10/2007 2:07	0.390255	0.075592	0.499129	0.472405	0.533652
28/10/2007 2:11	0.852175	0.458369	0.833909	0.829505	0.810293
28/10/2007 2:14	0.736747	0.555517	0.710522	0.70606	0.69788
28/10/2007 2:18	0.863811	0.500264	0.786445	0.777365	0.695859
28/10/2007 2:22	0.823195	0.621488	0.819111	0.814297	0.785244
28/10/2007 2:26	0.656638	0.497894	0.648256	0.653116	0.626999
28/10/2007 2:29	0.587194	0.450315	0.515451	0.498204	0.454882
28/10/2007 2:33	0.841178	0.740592	0.83624	0.833413	0.828193
28/10/2007 2:37	0.933038	0.76004	0.933919	0.93436	0.939976
28/10/2007 2:41	0.919843	0.868882	0.92163	0.92355	0.915143
28/10/2007 2:44	0.967918	0.950266	0.969089	0.96819	0.966122
28/10/2007 2:48	0.978558	0.970945	0.983599	0.983933	0.984988
28/10/2007 2:52	0.939291	0.95944	0.953044	0.952291	0.950052
28/10/2007 2:56	0.975708	0.931562	0.98261	0.981653	0.976193
28/10/2007 2:59	0.938855	0.938656	0.937962	0.936471	0.935679
Average	0.792748	0.684286	**0.794531**	0.790169	0.779514

Table 1 Root-mean-square-errors of MLP forecast and different CONN forecasts

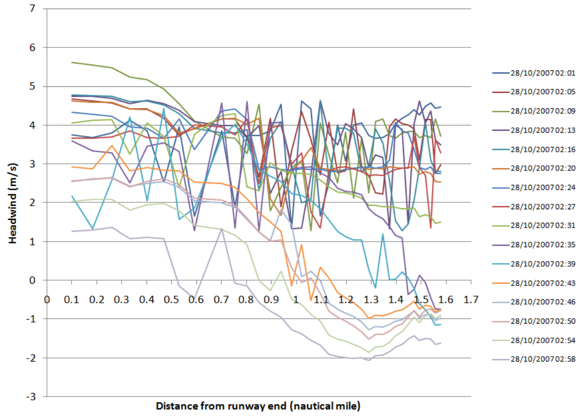

5 neurons

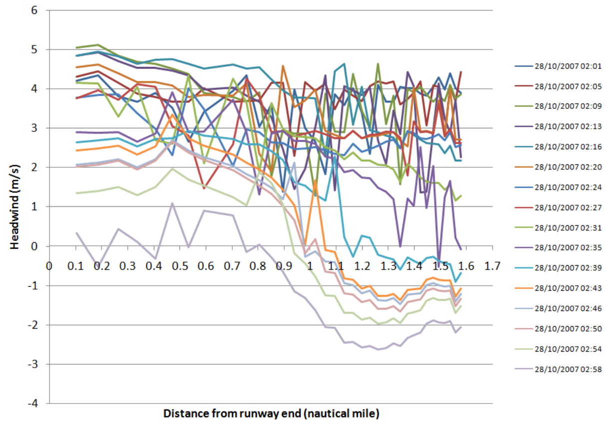

7 neurons

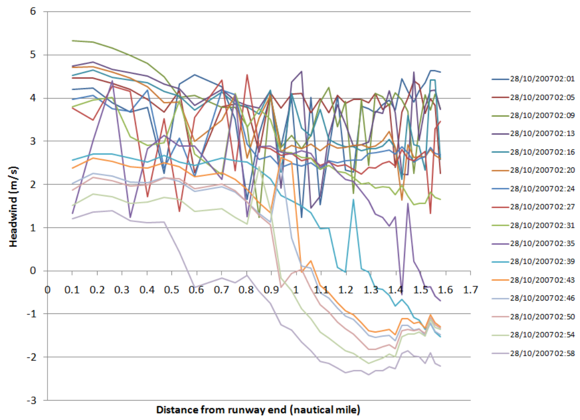

8 neurons

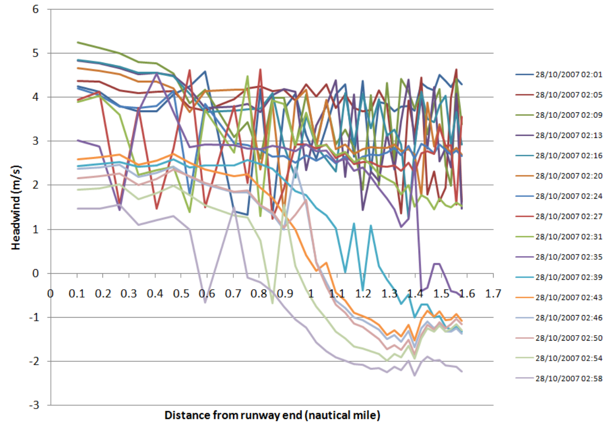

9 neurons

Figure 5 CONN forecasts with different number of neurons in the hidden layer

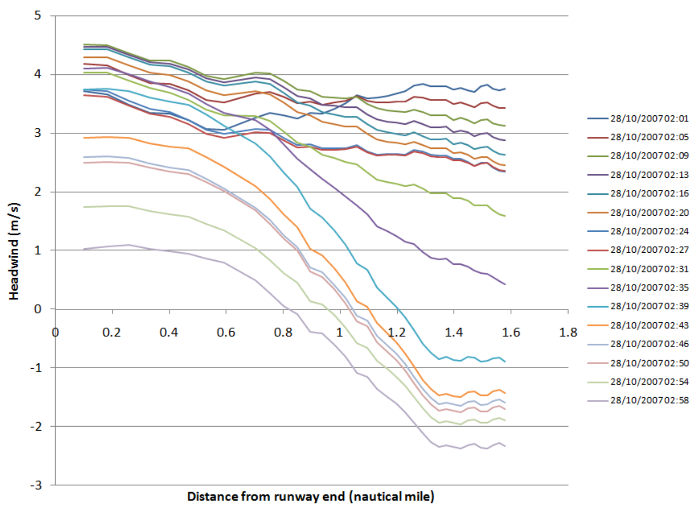

Figure 6 CONN forecast with non-sequential ordering of training dataset (according to time) as described in Section 6 of the main text

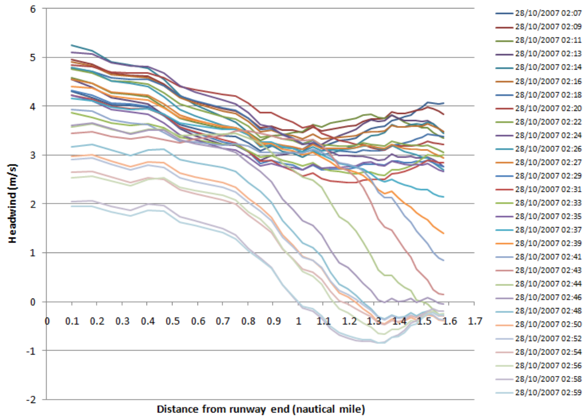

Skip 4

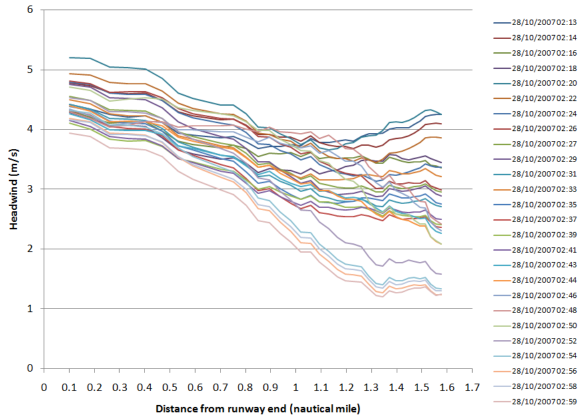

Skip 7

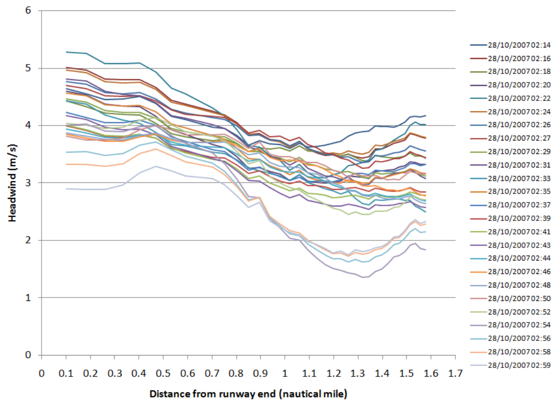

Sip 8

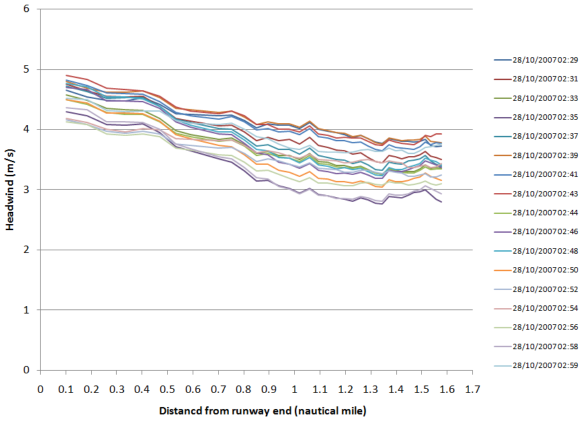

Skip 16

Figure 7 CONN forecasts with different number of scans being skipped between the training data and the forecast time